Nuclear export of the rate-limiting enzyme in phosphatidylcholine synthesis is mediated by its membrane binding domain[S]

Karsten Gehrig, Craig C. Morton, and Neale D. Ridgway[1]

Departments of Pediatrics, and Biochemistry & Molecular Biology, Atlantic Research Centre, Dalhousie University, Halifax, Nova Scotia, Canada

Abstract CTP:phosphocholine cytidylyltransferase α (CCTα), the rate-limiting enzyme in the CDP-choline pathway for phosphatidylcholine (PtdCho) synthesis, is activated by translocation to nuclear membranes. However, CCTα is cytoplasmic in cells with increased capacity for PtdCho synthesis and following acute activation, suggesting that nuclear export is linked to activation. The objective of this study was to identify which CCTα domains were involved in nuclear export in response to the lipid activators farnesol (FOH) and oleate. Imaging of CCT-green fluorescent protein (GFP) mutants expressed in CCTα-deficient CHO58 cells showed that FOH-mediated translocation to nuclear membranes and export to the cytoplasm required the membrane binding amphipathic helix (domain M). Nuclear export was reduced by a mutation that mimics constitutive phosphorylation of the CCT phosphorylation (P) domain. However, domain M alone was sufficient to promote translocation to the nuclear envelope and export of a nuclear-localized GFP construct in FOH- or oleate-treated CHO58 cells. In the context of acute activation with lipid mediators, nuclear export of CCT-GFP mutants correlated with in vitro activity but not PtdCho synthesis. This study describes a nuclear export pathway that is dependent on membrane interaction of an amphipathic helix, thus linking lipid-dependent activation to the nuclear/cytoplasmic distribution of CCTα.—Gehrig, K., C. C. Morton, and N. D. Ridgway. **Nuclear export of the rate-limiting enzyme in phosphatidylcholine synthesis is mediated by its membrane binding domain.** ***J. Lipid Res.*** **2009.** 50: **966–976.**

Supplementary key words CTP:phosphocholine cytidylyltransferase α • amphipathic helix • fatty acid • farnesol

Phosphatidylcholine (PtdCho) has essential roles in membrane structure, bile and lipoprotein secretion, cell proliferation, and apoptosis (1, 2). All mammalian cells synthesize PtdCho by the CDP-choline (Kennedy) pathway or by an alternate hepatic pathway involving sequential methylation of phosphatidylethanolamine (3). In addition to its central role in forming the limiting, semi-permeable membranes of cells and organelles, PtdCho is also a source of bioactive lipids such as phosphatidic acid, diacylglycerol (DAG) and FAs. The synthesis of PtdCho by the CDP-choline pathway is regulated by the rate-limiting enzyme CTP:phosphocholine cytidylyltransferase (CCT). Mammals express several structurally related CCT isoforms encoded by the CCTα and -β genes (4). CCTα is ubiquitously expressed in tissues and cultured cells, whereas the CCTβ isoforms display tissue-specific expression (5, 6). Isoforms encoded by these genes have highly conserved catalytic domains and 50-amino-acid amphipathic helices (termed domain M) that mediate reversible interaction with lipid bilayers (7). Domain M insertion into membranes is enhanced by type II lipids, such as phosphatidylethanolamine and DAG, or by negatively charged lipids, such as FAs and phosphatidylglycerol (8, 9). Membrane association of CCTα results in enhanced catalytic activity due to a reduced K_m for CTP (10). Adjacent to domain M is a phosphorylation (P) domain, which in human CCTα contains 16 putative serine phosphorylation sites that negatively regulate enzyme association with membranes (11, 12).

A distinguishing feature of CCTα is the presence of an N-terminal nuclear localization signal (NLS) that directs the enzyme to the nucleus in many cultured and primary cells (13–16). CCTβ isoforms lack an NLS and conse-

This research was supported by Canadian Institutes of Health Research Operating Grant MOP-62916. K.G. was the recipient of an Issac Walton Killiam Graduate Studentship. C.C.M. was the recipient of a Nova Scotia Health Research Foundation Studentship.

Manuscript received 8 December 2008 and in revised form 19 December 2008.

Published, JLR Papers in Press, December 20, 2008.
DOI 10.1194/jlr.M800632-JLR200

Abbreviations: CCT, cytidine triphosphate:phosphocholine cytidylyltransferase; DAG, diacylglycerol; ER, endoplasmic reticulum; FOH, farnesol; GFP, green fluorescent protein; INM, inner nuclear membrane; NE, nuclear envelope; NES, nuclear export signal; NLS, nuclear localization signal; NPC, nuclear pore complex; NR, nucleoplasmic reticulum; PtdCho, phosphatidylcholine.

[1] To whom correspondence should be addressed.
e-mail: nridgway@dal.ca

[S] The online version of this article (available at http://www.jlr.org) contains supplementary data in the form of three figures and two videos that are in supplementary Figs. I and III.

quently are found in the cytoplasm or associated with the endoplasmic reticulum (ER). In terms of PtdCho production, the functional significance of nuclear CCTα is unclear because the enzyme that supplies phosphocholine, choline kinase, is cytoplasmic (17) and the terminal enzymes that produce PtdCho, choline and choline-ethanolamine phosphotransferases, are localized to the Golgi apparatus and ER (18). Activation of nuclear CCTα by DAG or FAs results in translocation to the nuclear envelope (NE) (14, 15). This leads not only to stimulation of enzyme activity, but also to physical deformation of membranes due to insertion of domain M into one leaflet of the bilayer (19, 20). Membrane deformation by CCTα, which also requires nuclear lamins, results in double membrane invaginations of the NE, termed the nucleoplasmic reticulum (NR). Thus CCTα may have a role in defining nuclear membrane architecture in important pathological and developmental processes (21, 22), as well as coordinating PtdCho synthesis with cell cycle events (23).

CCTα is active in the nucleus and has nuclear-specific functions, but localization in the nucleus is not strictly required for survival of CHO cells (16). Furthermore, CCTα is constitutively cytoplasmic in cells with increased demand for PtdCho, such as primary hepatocytes (24), type II pneumocytes (25), and differentiating B cells (26). Exit of stationary cells into G_1 also caused export of CCTα from the nucleus (27), perhaps as a response to lipophilic activators, such as FAs and DAG, produced by PtdCho catabolism. In support of this conclusion, addition of exogenous farnesol (FOH) and oleyl alcohol, potent lipid activators of CCTα, induced rapid NE translocation and subsequent enzyme export to the cytoplasm (13, 28). These agents also induced apoptosis and caspase cleavage of the CCTα NLS. However, export of CCTα was not affected by caspase inhibition or mutagenesis of the CCTα caspase site, indicating that the export signal is related to membrane translocation and activation (13). Collectively, this implies that normally dividing cells can synthesize adequate amounts of PtdCho regardless of the site of CDP-choline synthesis, but that nuclear export of CCTα occurs in response to lipid activators and increased demand for PtdCho.

In this study, we used green fluorescent protein (GFP)-tagged CCTα to establish that the amphipathic helix domain M was necessary and sufficient to promote nuclear export by a mechanism that involved initial nuclear membrane translocation. Furthermore, activation of CCTα by oleate resulted in nuclear export that was reversed upon removal of the FA. These results are consistent with a model wherein the nuclear/cytoplasmic distribution of CCTα is regulated by domain M in response to the membrane content of lipid activators.

MATERIALS AND METHODS

CCT-GFP vectors

The monomeric form of GFP (L221K) encoded by pEGFP-N1 was used in all constructs (29). Vectors encoding CCT-3EQ-GFP, CCT-5KQ-GFP, and CCT-8KQ-GFP were previously described (20). Domain M fused to tandem copies of nuclear-localized GFP (M-2GFP-NLS) was created as follows. A region of CCTα encoding domain M (amino acids 237–310) was amplified (5′-GCCAAGGAGCTCAATGTCAGCAAGCTTATGGAAAAG-3′, 5′-GACTCTGCTTGGGACTGATGGCCCGCGGCATC-3′) and cloned into the *Hind*III and *Sac*II sites of pEGFP-N1 (Clontech, Palo Alto, CA). A triplet repeat encoding the SV40 NLS was then cloned into the *BsrG*I and *Not*I sites at the 3′ end of the construct. Finally, a cassette encoding an additional GFP flanked by *Apa*I and *Age*I sites was amplified (5′-CCCGGGATCCACGGGCCCCCACCATGGTGAGC-3′, 5′-CTAGAGTCGCGGCCGACCGGTTTGTACAGCTCGTCCATGCC-3′) and cloned into the construct to produce an in-frame tandem repeat of GFP. Domain M was excised from the construct to create the control vector encoding nuclear-localized GFP (2GFP-NLS).

Phosphorylation mutants CCT-16SA, CCT-16SE, CCT-7SA, and CCT-ΔP (CCT 1-314) [kindly provided by Dr. Claudia Kent (12)] were mutagenized to remove the stop codon and change the reading frame, cloned into pcDNA3.1-V5, digested with *Hind*III and *Sac*II, and ligated into pEGFP-N1. A similar approach was used to make a GFP construct with a deletion of domain M and P (CCT-ΔMP-GFP) using pCCT-Δ236 (19). Site-directed mutagenesis of pCCT-GFP was used to delete the region encoding domain M to produce pCCT-ΔM-GFP.

Cell culture and transfections

CHO58 cells expressing temperature-sensitive CCTα (30) were cultured at 33°C in an atmosphere of 5% CO_2 with DMEM plus 5% FBS and 34 μg proline/ml (medium A). CHO58 cells were transfected with CCT-GFP constructs using Lipofectamine 2000 reagent (Invitrogen, Burlington, ON). After 12–14 h at 37°C, cells were washed once, switched to serum-free DMEM or Ham's F-12 containing 10 mM HEPES (pH 7.4), and incubated at 40°C or 42°C for 1 h to suppress expression of endogenous temperature-sensitive CCTα. Cells were treated with FOH or oleate for the times and concentrations indicated in the figure legends, and either prepared for fluorescence microscopy or harvested for immunoblotting and enzyme assays.

Fluorescence microscopy and quantification of nuclear export

CHO58 cells were cultured to 70% confluence on glass coverslips, fixed in 4% paraformaldehyde for 15 min, and permeabilized in 0.05% (w/v) Triton X-100 at −20°C for 10 min. Cells were washed three times in PBS containing 1% (w/v) BSA and incubated for 20 min with 10 μg/ml Hoechst 33258 (Invitrogen). Following three washes in PBS, cells were mounted on glass slides using 10 μl of mowiol (Calbiochem, Gibbstown, NJ). Images were captured using a Zeiss Axiovert 200M fluorescence microscope equipped with an axioCam HRm CCD camera and 100× oil-immersion objective (NA 1.4).

To quantify nuclear and cytoplasmic localization of wild-type and mutant CCT-GFP, a threshold contrast/brightness setting was selected during image capture using Axiovision 4.5 that eliminated background cytoplasmic fluorescence in CHO58 cells expressing CCT-ΔMP-GFP. All other settings remained constant between experiments, and only cells with similar levels of fluorescence were chosen for quantitation. CCT-ΔMP-GFP-expressing cells were selected because this mutant is not membrane associated, and cells were devoid of cytoplasmic staining under untreated conditions. Images were exported to Photoshop, where a pixel threshold value was selected that eliminated cytoplasmic fluorescence in images of nontransfected CHO58 cells. This setting was determined in each experiment and applied to images of cells expressing wild-type and mutant CCT-GFPs treated with or without FOH. Next, nuclear and total pixels (expressed as area)

for Hoechst staining and GFP, respectively, were quantified using ImageJ (v1.38). Relative cytoplasmic GFP fluorescence was then expressed as total pixel area minus nuclear pixel area divided by total pixel area.

For live-cell imaging (**Fig. 1**), CHO58 cells were transiently transfected with CCT-GFP for 12–14 h, transferred to serum-free F-12 medium with 10 mM HEPES (pH 7.4), and mounted on the 40°C heated stage of a Nikon EclipseT2000-E inverted microscope equipped with a 100× oil-immersion objective (NA 1.4) and GFP filter set. After 1 h, cells were treated with FOH (60 μM) or oleate (320 μM)-BSA, and images were captured at 30 s intervals using a Photonics Cascade 512B CCD camera (Woburn, MA) and Metamorph software program (Universal Imaging, West Chester, PA). Live-cell images were taken on a Zeiss Axiovert 200M inverted microscope equipped with a 100× oil-immersion objective (NA 1.4), Zeiss axioCam HRm CCD camera and heated stage.

CCT assays and immunoblotting

CHO58 cells expressing CCT-GFP and various CCT-GFP mutants were cultured at 40°C or 42°C for 1 h prior to harvesting a 16,000 *g* supernatant fraction as previously described (20). CCT activity in this supernatant fraction was assayed using phospho [^{14}C]choline in the presence or absence of 2 mM PtdCho-oleic acid (1:1, mol/mol) liposomes or 2 mM PtdCho-FOH (3:2, mol/mol) liposomes (31). Enzyme activity was normalized to expression of individual CCT-GFP proteins in the supernatant fraction as determined by immunoblotting with an anti-GFP antibody and densitometry. Equivalency of protein loads was determined by immunoblotting with an actin polyclonal antibody.

RESULTS

CCT-GFP is exported from the nucleus in response to FOH

Similar to the endogenous enzyme, CCT-GFP is localized to the nucleus in CHO cells and undergoes translocation to the NE and NR in response to exogenous oleate (19, 20). This suggested that CCT-GFP could be used as a probe to monitor nuclear export following stimulation with FOH or oleate. To test this, CCT-GFP was transiently expressed for 12 h in CHO58 cells harboring a temperature-sensitive version of CCTα, transferred to a 40°C microscope stage, and images were captured at 30 s intervals following treatment with FOH (Fig. 1). CCT-GFP translocation to the NE and nuclear punctuate structures corresponding to the NR, as well as limited export to the cytoplasm, was observed 10–20 min after FOH treatment. After 30 min, CCT-GFP was localized to the cytoplasm in approximately 75% of cells (a Quicktime movie from which these pictures were taken is shown in supplementary Fig. I). Additional experiments showed that CHO58 cells treated with FOH for 45 min displayed >90% release of CCT-GFP to the cytoplasm and no evidence of chromatin condensation or other morphological changes related to apoptosis.

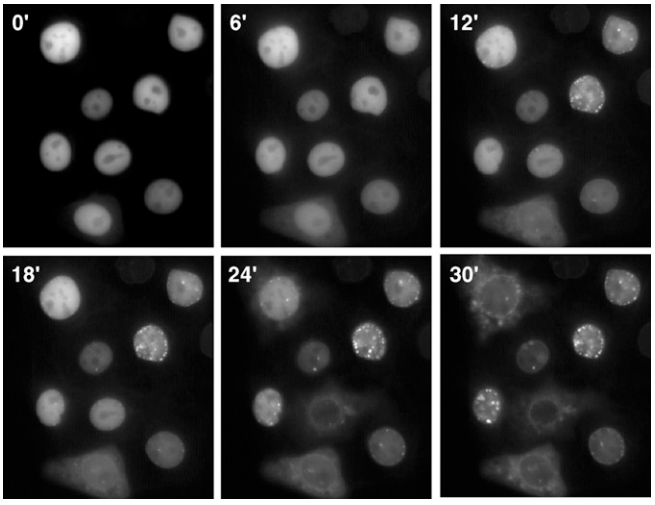

Fig. 1. Nuclear export of cytidine triphosphate:phosphocholine cytidylyltransferase-green fluorescent protein (CCT-GFP) in live cells. CHO58 cells transiently expressing CCT-GFP were mounted on a 40°C heated microscope stage. After equilibration for 15–20 min, cells received 60 μM farnesol (FOH), and images were captured at 30 s intervals (150 ms exposures) for 30 min as described in Materials and Methods. The Quicktime movie from which these individual images were extracted is shown in supplementary Fig. I.

Domain M is required for membrane translocation and nuclear export of CCT-GFP

CCT-GFP appeared to localize to the NE and NR prior to appearing in the cytoplasm (Fig. 1), suggesting that membrane localization was a prerequisite for export. Because translocation of CCTα to membranes is governed by domains M and P (11, 12, 32), various CCT truncation and point mutants in these domains were fused to GFP in order to monitor their activity and cellular localization in CHO58 cells after treatment with FOH or oleate. The series of CCT-GFP mutants used for these experiments is as follows (**Fig. 2A**): point mutations in domain M that affect affinity for membranes (CCT-3EQ, -5KQ, and -8KQ) (33); mutations of domain P that prevent or mimic phosphorylation (CCT-16SA, -16SE, and -7SA) (12); and deletion of domain M and/or P (CCT-ΔM, -ΔP, and -ΔMP). To assay in vitro activity, a low-speed supernatant fraction was isolated from CHO58 cells transiently expressing wild-type and mutant CCT-GFPs at the nonpermissive temperature to reduce endogenous CCTα activity. The supernatant fraction isolated from these cells contained soluble CCT-GFPs that migrated at the predicted molecular mass and were intact based on the absence of free GFP (Fig. 2B). The supernatant fractions were then assayed for CCT activity in the presence or absence of PtdCho-oleate or PtdCho-FOH liposomes (Fig. 2C). PtdCho-oleate liposomes activated CCT-GFP 5-fold, whereas PtdCho-FOH vesicles afforded a 2-fold activation. CCT-3EQ-GFP had elevated activity in the absence of oleate or FOH, consistent with the role of these interfacial glutamate residues in pH-dependent interaction with membranes (33). Lipid activators did not cause a further significant increase in activity. CCT-5KQ-GFP and CCT-8KQ-GFP have decreased catalytic activity using PtdCho vesicles containing 5–20% oleate (20), but vesicles containing 50% oleate significantly stimulated activity. PtdCho-FOH liposomes activated CCT-5KQ-GFP but not the 8KQ mutant. Consistent with the inhibitory role of domain P phosphorylation (12), the activity of CCT-16SA-GFP and CCT-7SA-GFP was elevated under basal conditions and stimulated by oleate and FOH. In contrast, CCT-16SE had lower

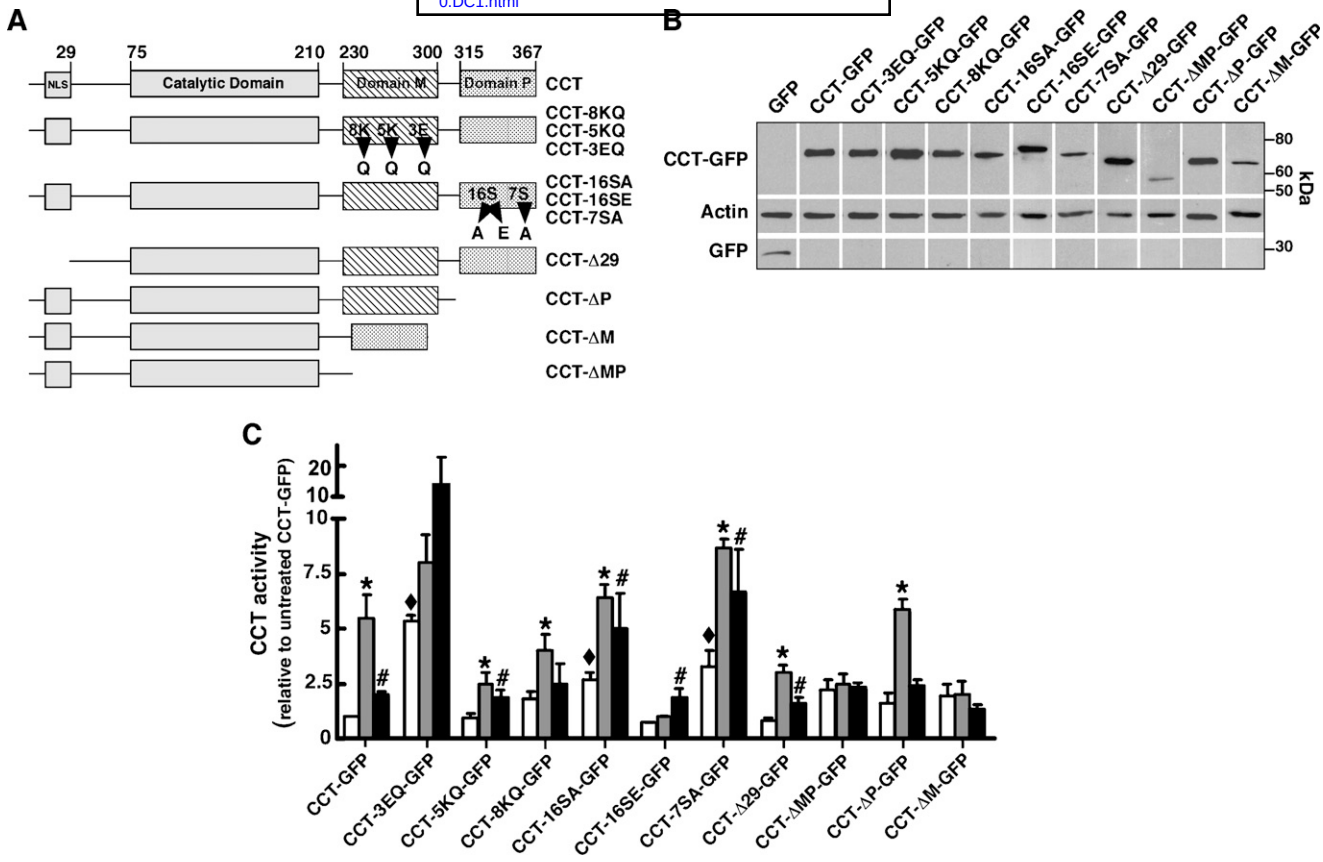

Fig. 2. In vitro activity and expression of CCT-GFP mutants. A: Domain structure of wild-type and CCTα mutants. GFP was fused to the C terminus of all constructs (not shown). B: CHO58 cells were transfected with CCT-GFP or the indicated mutants at 37°C for 12–14 h, shifted to 40°C or 42°C for 2 h and harvested, and 16,000 *g* supernatants were prepared and immunoblotted for GFP and actin. C: Enzyme activity was assayed in cell supernatants in the absence of lipid activators (open bars), with phosphatidylcholine (PtdCho)-oleate vesicles (1:1, mol/mol) (grey bars), or with PtdCho-FOH vesicle (3:2, mol/mol) (black bars) as described in Materials and Methods. Background CCT activity in supernatants from cells transfected with pEGFP was subtracted. Activity of wild-type and CCT mutants was normalized to expression of individual CCT-GFP proteins (measured by immunoblotting) and then expressed relative to activity under unstimulated conditions. CCT activity averaged 1,288, 1,091, and 1,217 dpm/assay in the supernatants of pEGFP-transfected cells without addition, plus oleate, or plus FOH, respectively. Activity averaged 1,653, 7,138, and 4,124 dpm/assay in supernatants from CCT-GFP-expressing cells with no addition, plus oleate, or plus FOH, respectively. Results are the mean and SEM of three separate experiments. $^{*}P < 0.05$ compared with corresponding unstimulated activity; $^{\#}P < 0.05$ compared with corresponding unstimulated activity; $\blacklozenge P < 0.05$ compared with unstimulated CCT-GFP.

basal activity, and was activated by FOH but not oleate. The basal activity of domain M deletion mutants CCT-ΔM-GFP and CCT-ΔMP-GFP was similar to control and not stimulated by oleate or FOH. The domain P deletion mutant was strongly activated by PtdCho-oleate vesicles but not FOH. Removal of the N-terminal NLS at the caspase cleavage site (CCT-Δ29-GFP) did not affect in vitro activity relative to wild-type. Collectively, CCT-3EQ-GFP, 16SA-GFP, and 7SA-GFP had significantly increased basal activity. CCT-8KQ-GFP, 16SE-GFP, and ΔP-GFP displayed a discrepancy in relative activation by oleate versus FOH, which could be related to the different charge and structure of these activators.

To assess the effect of these CCT mutations on PtdCho synthesis, transfected CHO58 cells were shifted to the nonpermissive temperature and [^{3}H]choline incorporation into PtdCho was measured in the absence and presence of oleate and normalized to expression of each mutant in whole-cell lysates (**Fig. 3**). Only in cells expressing CCT-GFP and CCT-5KQ-GFP was there significant activation of PtdCho synthesis by oleate. PtdCho synthesis in cells expressing CCT-3EQ-GFP was increased 25–40-fold, a much higher level of activation than observed in vitro (Fig. 2C). Similar to in vitro conditions, CCT-16SE-GFP-expressing cells had a low level of PtdCho synthesis that was not activated by oleate. In general, however, PtdCho biosynthesis did not reflect the basal or oleate-stimulated activity of various CCT-GFP mutants predicted by in vitro assays. A comparison of PtdCho synthesis to in vitro activity of CCT-GFP mutants in the presence of FOH could not be made because FOH induces a rapid block in conversion of CDP-choline to PtdCho in numerous cell types (13, 34).

As shown in Fig. 1, FOH can be used to stimulate CCT translocation and export from the nucleus. Unlike oleate, FOH is poorly metabolized and thus provides a consistent stimulus for CCTα activation and export. To identify mutants with defective nuclear export, CHO58 cells were transiently transfected with CCT-GFP constructs and cultured in the absence or presence of FOH, and GFP fluorescence and nuclear staining (Hoechst 33258) were monitored by fluorescence microscopy (**Fig. 4**; a full set of single and

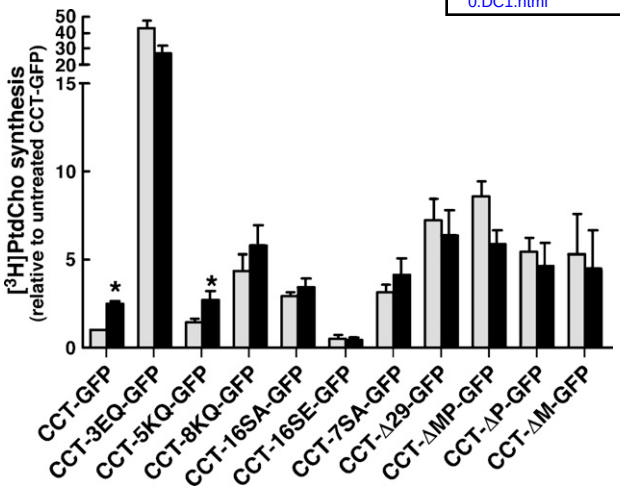

Fig. 3. PtdCho synthesis in CHO58 cells expressing CCT-GFP mutants. CHO58 cells were transfected with CCT-GFP or the indicated mutants as described in the legend to Fig. 2. After 2 h at 42°C, cells were incubated with choline-free DMEM containing [^{3}H]choline (2 μCi/ml) for 1 h, followed by treatment without (grey bars) or with (black bars) 300 μM oleate/complexed with BSA for 1 h. [^{3}H] PtdCho was measured and normalized to expression of individual CCT-GFP proteins by immunoblotting of whole-cell lysates, and expressed relative to synthesis in unstimulated CHO58 cells transfected with CCT-GFP. Background [^{3}H]PtdCho synthesis in cells transfected with pEGFP was subtracted. Total PtdCho synthesis was 1,045 and 910 dpm/dish in control and oleate-treated pEGFP-transfected cells, respectively. Total PtdCho synthesis was 13,655 and 36,550 dpm/dish in control and oleate-treated CCT-GFP-expressing cells, respectively. $*P < 0.05$ compared with corresponding unstimulated control. Results are the mean and SEM of three separate experiments.

merged images for all untreated cells is shown in supplementary Fig. II). To confirm that export was specific for CCT-GFP and not due to disruption of the NE, it was necessary to demonstrate that a soluble nuclear protein with a molecular mass above the diffusion limit of the nuclear pore complex (NPC) did not exit the nucleus in response to FOH. A 60 kDa protein containing tandem GFPs fused to the SV40 NLS (2GFP-NLS) was expressed in the nucleoplasm and did not export during FOH treatment for 45 min (Figs. 4A, 6D). In contrast, CCT-GFP was extensively localized in the cytoplasm following exposure to FOH (Fig. 4A). This indicated that release of CCT-GFP to the cytoplasm did not result from permeabilization of the NE or disruption of nuclear pores by FOH. The proportion of CCT-GFP in the cytoplasm of FOH-treated cells was similar to CCT-Δ29-GFP, which was primarily cytoplasmic owing to removal of the NLS (Fig. 4A). CCT-GFPs with point mutations in domain M were translocated to the NE but displayed varying levels of fluorescence in the nucleoplasm, NE, and cytoplasm (Fig. 4B). The enhanced membrane affinity of CCT-3EQ-GFP resulted in variable punctuate fluorescence in the cytoplasm and nucleus in the absence and presence of FOH (Fig. 4B). Mutants with compromised membrane binding (CCT-5KQ-GFP and CCT-8KQ-GFP) translocated to the NE and NR, but export to the cytoplasm was reduced compared with CCT-GFP. Domain P phosphorylation mutants appeared to be exported to the cytoplasm to a similar extent as CCT-GFP (Fig. 4C). Deletion of domain M (CCT-ΔMP-GFP and CCT-ΔM-GFP), but not domain P (CCT-ΔP-GFP), prevented cytoplasmic localization in response to FOH (Fig. 4D). To ensure that wild-type and mutant CCT-GFPs remained intact during FOH treatment, the expression of each mutant shown in Fig. 4A–D was evaluated by SDS-PAGE and immunoblotting of total lysates from cells treated with and without FOH (Fig. 4E). Free GFPs were not detected in cells expressing CCT-GFPs, nor did exposure of cells to FOH induce caspase cleavage at the N-terminus.

To quantify the extent of nuclear export of wild-type and CCT-GFP mutants shown in Fig. 4, cytoplasmic fluorescence was measured as pixel area and expressed relative to total cellular fluorescence (**Fig. 5**). This method quantifies fluorescence based on the absence or presence of pixels in the cytoplasm above a threshold value. Quantification of cytoplasmic and nuclear fluorescence revealed that almost 75% of CCT-GFP was exported from the nucleus in response to FOH, a value that was similar to the cytoplasmic distribution of CCT-Δ29-GFP. Cytoplasmic CCT-3EQ-GFP was quite variable in untreated cells and was further increased by FOH to a level similar to CCT-GFP. The reduced membrane affinity of CCT-5KQ-GFP and CCT-8KQ-GFP resulted in significant reduction in export. CCT-GFP domain P mutants with serine-to-alanine mutations (16SA and 7SA) were exported to a similar extent as CCT-GFP, but the cytoplasmic proportion of CCT-GFP-16SE, a mutant mimicking constitutive phosphorylation, was significantly reduced. Removal of domain M, either by truncation at amino acid 236 (CCT-ΔMP-GFP) or by deletion of the entire amphipathic helix (CCT-ΔM-GFP), resulted in low cytosolic fluorescence under control conditions and only 10–15% export in the presence of FOH. CCT-ΔP-GFP was exported to a greater degree than the other two deletion mutants but less than CCT-GFP. This could be related to poor activation of this mutant by FOH in vitro (Fig. 2C). Collectively, the results indicate that domain M is necessary for FOH-mediated membrane translocation of CCTα and subsequent export from the nucleus. However, export appeared to be negatively regulated by domain P phosphorylation.

Domain M is necessary and sufficient for nuclear export of CCT-GFP

To assess whether domain M was both necessary and sufficient to promote nuclear export, a reporter was constructed containing domain M (amino acids 236–310) fused with two copies of GFP (to prevent passive diffusion through the NPC) followed by a C-terminal SV40 NLS (M-2GFP-NLS) (**Fig. 6A**). CHO58 cells were transiently transfected with this construct and treated with FOH, and total cell lysates were subjected to SDS-PAGE and immunoblotting (Fig. 6B). 2GFP-NLS had the predicted molecular mass of 60 kDa, and a small amount of free GFP (30 kDa) was detected. M-2GFP-NLS had the expected molecular mass of 70 kDa, as well as additional proteins at 60 kDa and 65 kDa. These two proteins are probably the result of cleavage in domain M or at the GFP-domain M junction because the 60 kDa protein comigrated with 2GFP-NLS, and M-2GFP-

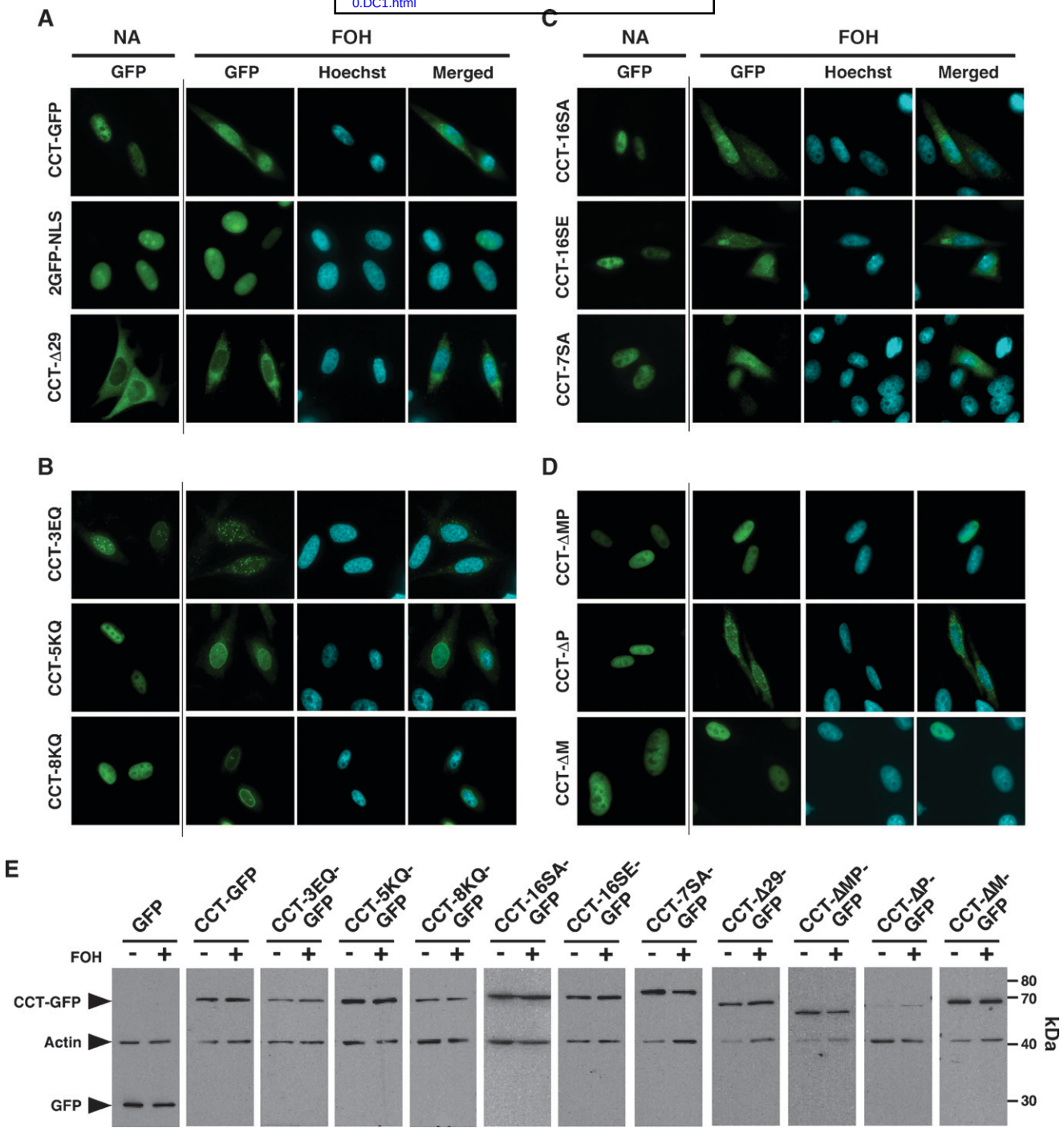

Fig. 4. Localization of wild-type and CCT-GFP mutants in FOH-treated CHO58 cells. Vectors encoding CCT-GFP or the indicated mutant proteins were expressed in CHO58 cells for 14 h, and shifted to 40°C for 1 h prior to stimulation with 60 μM FOH. After 45 min, cells were fixed and GFP and the nucleus (Hoechst staining) were visualized. A: CCT-GFP and nuclear 2GFP-nuclear localization signal (2GFP-NLS) and cytoplasmic (CCT-Δ29-GFP)-localized controls. B: Domain M point mutants (CCT-8KQ-GFP, -5KQ-GFP, and -3EQ-GFP). C: Phosphorylation mutants (CCT-16SA-GFP, -16SE-GFP, and -7SA-GFP). D: Domain M and P truncation mutants (CCT-ΔM-GFP, -ΔP-GFP, and -ΔMP-GFP). E: Total cell lysates prepared from CHO58 cells, transfected and treated with FOH as described above, were resolved by SDS-PAGE and immunoblotted for GFP and actin.

NLS fluorescence was entirely nuclear, indicating that the NLS was intact (see Fig. 6C, D). Imaging by confocal (Fig. 6C) or wide-field (Fig. 6D) microscopy showed that 2GFP-NLS and M-2GFP-NLS were diffusely localized in the nucleus or concentrated in several intranuclear structures. FOH treatment for 45 min did not change 2GFP-NLS localization. However, M-2GFP-NLS was translocated to the NE, and a majority of cells displayed significant export to the cytoplasm. Quantitation of fluorescence distribution (Fig. 6E) revealed that 15% of 2GFP-NLS was cytoplasmic in CHO58 cells treated with or without FOH. In contrast, cytoplasmic M-2GFP-NLS fluorescence was undetected in

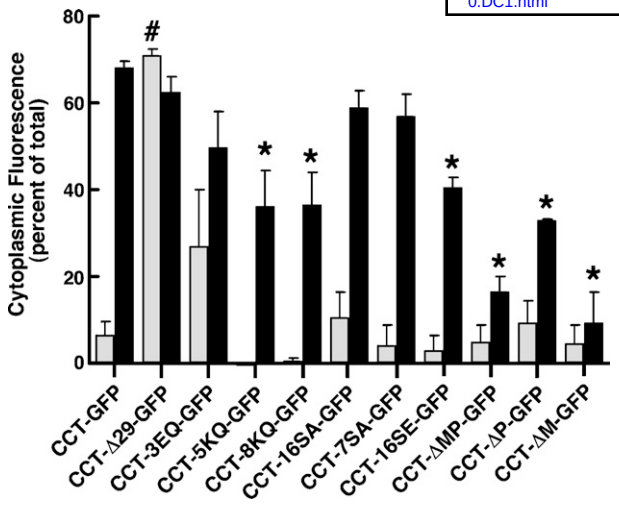

Fig. 5. Quantification of nuclear export reveals a role for domain M. Vectors encoding wild-type and mutant CCT-GFP were transfected in CHO58 cells for 14 h and imaged following FOH treatment as described in the legend to Fig. 4. The percent distribution of GFP fluorescence in the cytoplasm of at least 20 control (grey bars) and FOH-treated (black bars) cells was quantified for each GFP fusion protein as described in Materials and Methods. $^{*}P < 0.05$ compared with FOH treated CCT-GFP; $^{\#}P < 0.05$ compared with untreated CCT-GFP cells. Results are the mean and SEM of three separate experiments.

untreated cells and >50% was exported in response to FOH, a value similar to CCT-GFP. Thus, domain M is sufficient to promote membrane translocation and export of nuclear-localized GFP.

Export of proteins from the nucleus requires a large family of exportins, of which CRM1 has the broadest substrate range through recognition of leucine-rich nuclear export signals (NESs). To determine whether CRM1 was involved in CCT-GFP export, CHO58 cells transiently expressing CCT-GFP or M-2GFP-NLS were treated with leptomycin B, a CRM1 inhibitor (35), prior to activation of export by FOH. Leptomycin B (10–100 nM) had no effect on nuclear export, and a leucine-rich export signal (36) was not identified in domain M, further indicating that CRM1 is not involved (results not shown).

Oleate promotes membrane translocation and nuclear export of CCT-GFP

Nuclear export of endogenous CCTα and CCT-GFP by FOH is very rapid and occurs prior to apoptosis (13) (Fig. 1) and thus could be a general response to physiological activators. To test this, CHO58 cells transiently expressing CCT-GFP and M-2GFP-NLS were treated with oleate, a well-described CCTα activator that promotes translocation to the NE and NR (19), and live cells were viewed by fluorescence microscopy (**Fig. 7A**). Live-cell imaging was necessary because it was difficult to predict when CCT-GFP export would occur over a 30 min treatment, and export was transient owing to oleate metabolism at later time points. As a control, the localization of CCT-ΔM-GFP, a mutant that did not export in response to FOH (Figs. 4, 5), was monitored in oleate-treated cells. After exposure of cells to 300 μM oleate for 5 min and 10 min, CCT-GFP and M-2GFP-NLS fluorescence was decreased in the nucleus and increased in the cytoplasm of >90% of cells. During treatment with oleate, CCT-ΔM-GFP nuclear fluorescence remained constant, and there was little evidence of cytoplasmic localization (<10% of cells displayed cytoplasmic fluorescence).

We next determined whether oleate-mediated export of CCT-GFP was a reversible process. Individual cells that exported CCT-GFP after exposure to oleate for 5–10 min were identified and then switched into oleate-free medium containing 0.2% BSA (Fig. 7B). Imaging of these cells revealed that oleate promoted rapid translocation of CCT-GFP to the NR and NE, which subsequently diminished in intensity as cytoplasmic fluorescence increased. The replacement of oleate-containing media with media containing BSA after 6 min resulted in rapid import of CCT-GFP into the nucleus and dissociation of CCT-GFP from the NR and NE. After a 9 min washout period, CCT-GFP had assumed a diffuse nucleoplasmic distribution that was indistinguishable from untreated cells. A Quicktime movie showing the entire sequence of oleate stimulation and removal is shown in supplementary Fig. III.

DISCUSSION

CCTα is effectively separated from the other two enzymes of the CDP-choline pathway by the NE, a barrier that could be overcome by enzyme or substrate relocation. Here we have shown that transfer of CCTα from the nuclear to the cytoplasmic compartment requires nuclear membrane translocation and activation, and is mediated by domain M. This defines a novel, membrane-regulated nuclear export pathway that links CCTα activation with nuclear export, a condition that could apply in cells with increased demand for PtdCho.

Previously reported membrane affinities and in vitro activities (Fig. 2C) of CCT with point mutations in domains M and P were correlated with their cytoplasmic/nuclear distribution following FOH treatment (Figs. 4, 5). CCT-5KQ and -8KQ have reduced membrane affinity and activity due to disruption of basic residues involved in electrostatic interaction with anionic phospholipids (20, 33). Partial elimination of basic residues in CCT-5KQ-GFP did not affect activation by FOH. However, the more severely attenuated 8KQ mutant was not significantly activated. Both mutants displayed cytoplasmic export and appeared to be more prominently localized to the NE (Fig. 4B), suggesting that in the context of a more complex lipid environment, export following membrane attachment was impaired. Increased membrane affinity of CCT-3EQ resulted in variable cytoplasmic localization in untreated cells that was further enhanced by addition of FOH. The steady-state distribution of CCT-3EQ in untreated CHO cells could represent a situation in which the enzyme is not imported into the nucleus owing to constitutive attachment to the ER or outer NE, or is actively exported from the nucleus. Regardless, this distribution of CCT-3EQ supports the conclusion that membrane binding and activation favor cytoplasmic localization. Do-

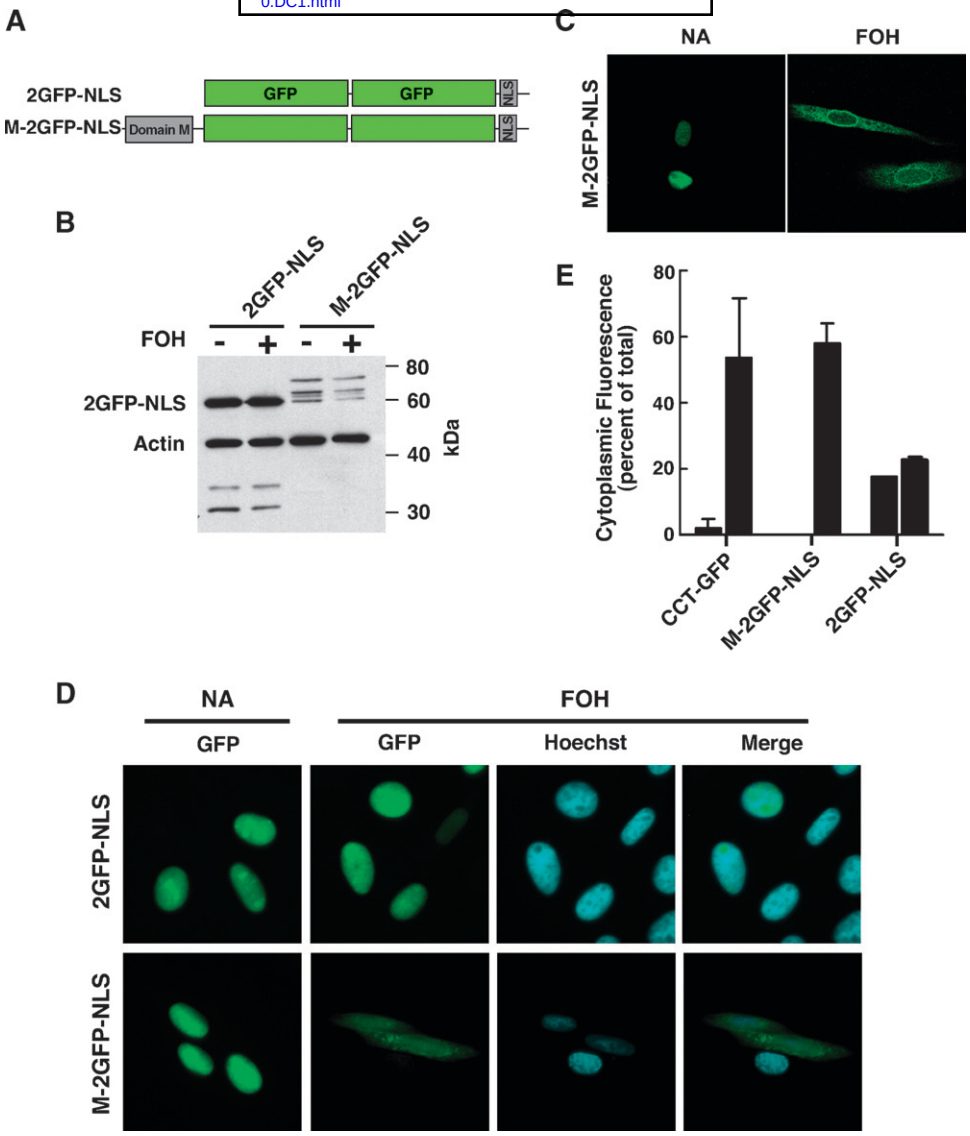

Fig. 6. Domain M is necessary and sufficient for nuclear membrane translocation and export. A: Tandem repeats of GFP were targeted to the nucleus by attachment of the SV40 NLS (2GFP-NLS). Domain M was attached to the N terminus to make the M-2GFP-NLS construct. B: Total lysates of CHO58 cells transiently expressing 2GFP-NLS or M-2GFP-NLS for 14 h and treated with or without 60 μM FOH for 45 min were immunoblotted for GFP and actin. C: Confocal imaging of M-2GFP-NLS in CHO58 cells treated with and without 60 μM FOH for 45 min. D: Wide-field fluorescence micrographs of M-2GFP-NLS or 2GFP-NLS exposed to 60 μM FOH for 45 min. The nucleus was visualized by Hoechst staining. E: Quantification of the cytoplasmic distribution of CCT-GFP, 2GFP-NLS, and M-2GFP-NLS fluorescence in control (grey bars) and FOH-treated (black bars) cells shown in D. Results are the mean and SEM of three separate experiments that involved analysis of at least 20 cells each.

main P has a subtle, inhibitory role in modifying membrane interaction that was speculated to involve interaction between phosphoserines and basic residues in domain M (11, 37). Consistent with the hyperphosphorylated state having reduced affinity for membranes, export of the constitutively phosphorylated mimic CCT-16SE was significantly reduced by 30%, and dephosphorylated CCT-16SA and -7SA had export indices that were similar to those of control. However, all three of these phosphorylation mutants were activated by FOH in vitro. Deletion of domain P (CCT-ΔP-GFP) caused reduced export, which was unexpected because domain M was available for membrane translocation. However, this mutant was not activated by FOH in vitro but retained activation by oleate, suggesting differential sensitivity to charged versus neutral lipid activators.

The results described above for domains M and P point mutants were rather inconclusive because the enzymes were activated by FOH under in vitro conditions but had a partial reduction in nuclear export. However, severely attenuated nuclear export and insensitivity of CCT-ΔM-GFP and CCT-ΔMP-GFP to FOH in vitro suggested that domain M was directly involved in export. To further demonstrate that domain M was both necessary and sufficient for nuclear membrane translocation and export, it was fused to tandem

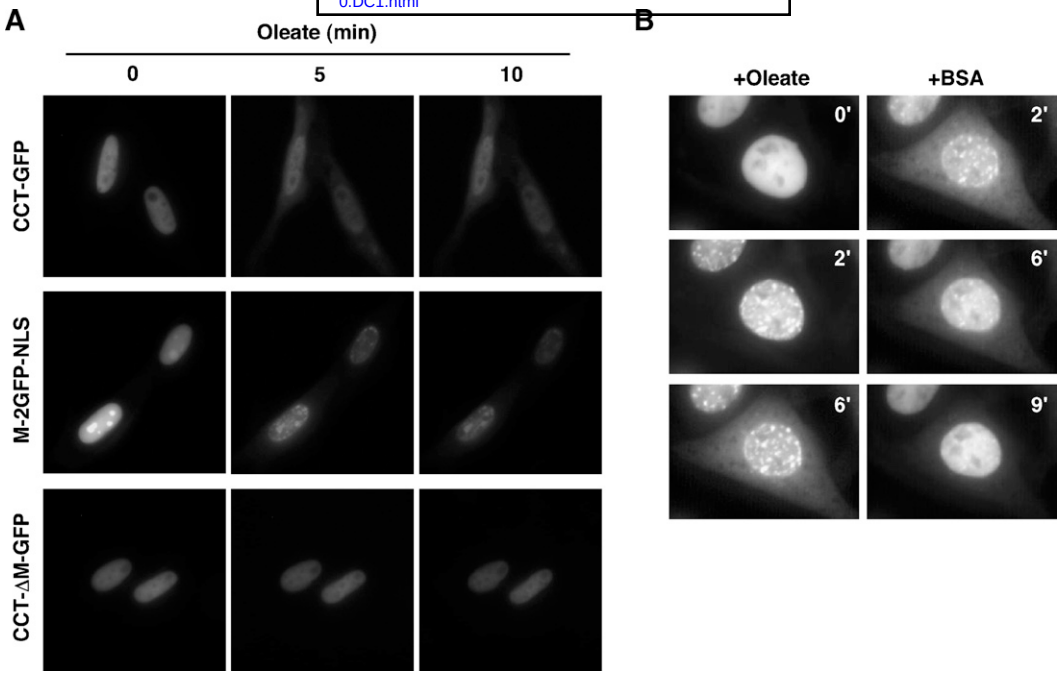

Fig. 7. Oleate promotes domain M-dependent export of CCT-GFP. A: CHO58 cells expressing CCT-GFP, CCT-ΔM-GFP, or M-2GFP-NLS were prepared for live-cell imaging as described in Materials and Methods. Cells were mounted on a 37°C heated stage and treated with an oleate-BSA complex (300 μM oleate), and images were captured (750 ms exposures) at the indicated times. B: CHO58 cells expressing CCT-GFP were treated with oleate (320 μM complexed with BSA) at 40°C, and images were captured (150 ms exposures) at 30 s intervals for 6 min. Cells that displayed significant nuclear export of CCT-GFP were identified, and medium was replaced with prewarmed (40°C) oleate-free F-12 medium containing 0.2% BSA. Images were captured for a further 9 min. The Quicktime movie from which these images were taken is shown in supplementary Fig. III.

repeats of GFP and directed to the nucleus with the SV40 NLS. In the presence of FOH, the localization and export index for M-2GFP-NLS was similar to that of CCT-GFP, indicating that domain M alone mediates this membrane translocation-dependent export pathway (Fig. 6E). To our knowledge, this is the first demonstration of a nuclear protein export pathway that is triggered by membrane recruitment of an amphitropic protein. The process is all the more novel because membrane translocation of CCTα also leads to enzyme activation, indicating that binding of CCTα to the inner nuclear membrane (INM) couples export with increased enzyme activity but not necessarily increased PtdCho synthesis. Identification of a nuclear import pathway for integral membrane proteins provides some insight into possible modes of CCTα export from the INM. Nuclear import of integral membrane proteins involves lateral diffusion along the nuclear pore membrane, eventual localization to the INM, and immobilization by interaction with the lamina (38, 39). Transfer through the NPC required karyopherins (40) and ATP (38) and was restricted to proteins with cytosolic domains <75 kDa (38). Passage of CCTα through the NPC presumably requires a karyopherin because the soluble portion of a CCTα dimer would be approximately 60 kDa, above the exclusion limit for passive diffusion of soluble cargo (41) but below that for integral membrane proteins. However, the karyopherin is not CRM1, because CCT-GFP export was leptomycin B-insensitive and domain M does not contain an obvious leucine-rich NES. We cannot rule out the possibility that CCTα export is NPC-independent, involving direct movement between the inner and outer nuclear membranes by vesicular trafficking or transient membrane fusion. It is noteworthy that both of these processes were ruled out for the nuclear import of integral membrane proteins (38).

Our conclusion that nuclear export of CCTα is facilitated by domain M translocation to the INM is consistent with cytoplasmic localization of the enzyme in cells with increased PtdCho and membrane synthesis. CCTα is partially or exclusively cytoplasmic in cells actively involved in secretion of PtdCho (24, 25, 42) or proliferation of intracellular membranes (26). Similarly, the burst of phospholipid degradation during the G_0–G_1 transition is accompanied by CCTα activation and nuclear export (27). Based on results using acute stimulation of CCTα with exogenous activators, we propose that cells with increased demand for PtdCho have endogenous lipid activators or altered membrane composition that favors sustained CCTα activation at the INM and subsequent export from the nucleus. Cytoplasmic localization of CCTα would favor enhanced PtdCho production, perhaps by more-efficient metabolic channeling with choline kinase and choline phosphotransferase.

It is important to note that acute stimulation with oleate and subsequent domain M-dependent nuclear export was

not correlated with PtdCho synthesis. PtdCho synthesis in cells expressing either constitutively nuclear or cytoplasmic CCT mutants was very similar and increased relative to CCT-GFP. CCT-ΔM-GFP was not exported from the nucleus in response to FOH or oleate, nor was it activated in vitro, yet it restored PtdCho synthesis in CHO58 cells. Although this suggests that PtdCho synthesis is not affected by CCTα localization, it is also possible that the mutations that trap CCT-GFP in these compartments also affect activity. For instance, deletion of domain M produces a constitutively active enzyme that is independent of lipid regulators (43), and deletion of the NLS (CCT-Δ29-GFP) would remove a recently identified lipid binding motif involved in CCT-dependent cross-bridging of membranes (44). Another confounding factor is that export occurs in 10–20 min and is reversible, whereas PtdCho synthesis was measured over 60 min. Thus, monitoring net PtdCho synthesis may not be sensitive enough to detect rapid and reversible changes in CCTα localization.

The identity of the physiological lipid activator(s) that promote nuclear CCTα activation and export is unknown. A study that examined production of lipid activators during the G_0–G_1 transition in IIC9 cells concluded that DAG was involved in CCTα activation (45). CCTα activation and cytoplasmic localization were also accompanied by increased DAG mass and lipin1 expression in differentiating B cells (26). Because lipin1 is partially nuclear (46), this identifies a potential site for activation of CCTα through localized production of DAG.

These studies identify a nuclear export pathway for CCTα that is linked to translocation and activation at nuclear membranes. Not only is the domain M amphipathic helix required for enzyme activation and deformation of membranes, it now has an important role in altering the intracellular site of CCTα activity from the nucleus to the cytoplasm. Because M-2GFP-NLS behaves like the full-length enzyme, this reporter construct could be potentially useful in identifying the endogenous lipids involved in CCT activation and in reporting their content in membranes of living cells.

Robert Zwicker provided excellent technical assistance. Xiaohui Zha (Ottawa Health Research Institute, Ottawa, ON) assisted with live-cell imaging.

REFERENCES

1. Vance, J. E., and D. E. Vance. 2005. Metabolic insights into phospholipid function using gene-targeted mice. *J. Biol. Chem.* **280:** 10877–10880.
2. Cui, Z., and M. Houweling. 2002. Phosphatidylcholine and cell death. *Biochim. Biophys. Acta.* **1585:** 87–96.
3. Vance, D. E., Z. Li, and R. L. Jacobs. 2007. Hepatic phosphatidylethanolamine N-methyltransferase, unexpected roles in animal biochemistry and physiology. *J. Biol. Chem.* **282:** 33237–33241.
4. Lykidis, A., and S. Jackowski. 2001. Regulation of mammalian cell membrane biosynthesis. *Prog. Nucleic Acid Res. Mol. Biol.* **65:** 361–393.
5. Karim, M., P. Jackson, and S. Jackowski. 2003. Gene structure, expression and identification of a new CTP:phosphocholine cytidylyltransferase beta isoform. *Biochim. Biophys. Acta.* **1633:** 1–12.
6. Lykidis, A., I. Baburina, and S. Jackowski. 1999. Distribution of CTP: phosphocholine cytidylyltransferase (CCT) isoforms. Identification of a new CCTbeta splice variant. *J. Biol. Chem.* **274:** 26992–27001.
7. Cornell, R. B. 1998. How cytidylyltransferase uses an amphipathic helix to sense membrane phospholipid composition. *Biochem. Soc. Trans.* **26:** 539–544.
8. Davies, S. M., R. M. Epand, R. Kraayenhof, and R. B. Cornell. 2001. Regulation of CTP:phosphocholine cytidylyltransferase activity by the physical properties of lipid membranes: an important role for stored curvature strain energy. *Biochemistry.* **40:** 10522–10531.
9. Attard, G. S., R. H. Templer, W. S. Smith, A. N. Hunt, and S. Jackowski. 2000. Modulation of CTP:phosphocholine cytidylyltransferase by membrane curvature elastic stress. *Proc. Natl. Acad. Sci. USA.* **97:** 9032–9036.
10. Yang, W., K. P. Boggs, and S. Jackowski. 1995. The association of lipid activators with the amphipathic helical domain of CTP:phosphocholine cytidylyltransferase accelerates catalysis by increasing the affinity of the enzyme for CTP. *J. Biol. Chem.* **270:** 23951–23957.
11. Yang, W., and S. Jackowski. 1995. Lipid activation of CTP:phosphocholine cytidylyltransferase is regulated by the phosphorylated carboxyl-terminal domain. *J. Biol. Chem.* **270:** 16503–16506.
12. Wang, Y., and C. Kent. 1995. Effects of altered phosphorylation sites on the properties of CTP:phosphocholine cytidylyltransferase. *J. Biol. Chem.* **270:** 17843–17849.
13. Lagace, T. A., J. R. Miller, and N. D. Ridgway. 2002. Caspase processing and nuclear export of CTP:phosphocholine cytidylyltransferase alpha during farnesol-induced apoptosis. *Mol. Cell. Biol.* **22:** 4851–4862.
14. Watkins, J. D., and C. Kent. 1992. Immunolocalization of membrane-associated CTP:phosphocholine cytidylyltransferase in phosphatidylcholine-deficient Chinese hamster ovary cells. *J. Biol. Chem.* **267:** 5686–5692.
15. Wang, Y., T. D. Sweitzer, P. A. Weinhold, and C. Kent. 1993. Nuclear localization of soluble CTP:phosphocholine cytidylyltransferase. *J. Biol. Chem.* **268:** 5899–5904.
16. Wang, Y., J. I. MacDonald, and C. Kent. 1995. Identification of the nuclear localization signal of rat liver CTP:phosphocholine cytidylyltransferase. *J. Biol. Chem.* **270:** 354–360.
17. Aoyama, C., H. Liao, and K. Ishidate. 2004. Structure and function of choline kinase isoforms in mammalian cells. *Prog. Lipid Res.* **43:** 266–281.
18. Henneberry, A. L., M. M. Wright, and C. R. McMaster. 2002. The major sites of cellular phospholipid synthesis and molecular determinants of fatty acid and lipid head group specificity. *Mol. Biol. Cell.* **13:** 3148–3161.
19. Lagace, T. A., and N. D. Ridgway. 2005. The rate-limiting enzyme in phosphatidylcholine synthesis regulates proliferation of the nucleoplasmic reticulum. *Mol. Biol. Cell.* **16:** 1120–1130.
20. Gehrig, K., R. B. Cornell, and N. D. Ridgway. 2008. Expansion of the nucleoplasmic reticulum requires the coordinated activity of lamins and CTP:phosphocholine cytidylyltransferase α. *Mol. Biol. Cell.* **19:** 237–247.
21. McClintock, D., L. B. Gordon, and K. Djabali. 2006. Hutchinson-Gilford progeria mutant lamin A primarily targets human vascular cells as detected by an anti-lamin A G608G antibody. *Proc. Natl. Acad. Sci. USA.* **103:** 2154–2159.
22. Brandt, A., F. Papagiannouli, N. Wagner, M. Wilsch-Brauninger, M. Braun, E. E. Furlong, S. Loserth, C. Wenzl, F. Pilot, N. Vogt, et al. 2006. Developmental control of nuclear size and shape by Kugelkern and Kurzkern. *Curr. Biol.* **16:** 543–552.
23. Jackowski, S. 1994. Coordination of membrane phospholipid synthesis with the cell cycle. *J. Biol. Chem.* **269:** 3858–3867.
24. Houweling, M., Z. Cui, C. D. Anfuso, M. Bussiere, M. H. Chen, and D. E. Vance. 1996. CTP:phosphocholine cytidylyltransferase is both a nuclear and cytoplasmic protein in primary hepatocytes. *Eur. J. Cell Biol.* **69:** 55–63.
25. Ridsdale, R., I. Tseu, J. Wang, and M. Post. 2001. CTP:phosphocholine cytidylyltransferase alpha is a cytosolic protein in pulmonary epithelial cells and tissues. *J. Biol. Chem.* **276:** 49148–49155.
26. Fagone, P., R. Sriburi, C. Ward-Chapman, M. Frank, J. Wang, C. Gunter, J. W. Brewer, and S. Jackowski. 2007. Phospholipid biosynthesis program underlying membrane expansion during B-lymphocyte differentiation. *J. Biol. Chem.* **282:** 7591–7605.
27. Northwood, I. C., A. H. Tong, B. Crawford, A. E. Drobnies, and R. B. Cornell. 1999. Shuttling of CTP:phosphocholine cytidylyltransferase between the nucleus and endoplasmic reticulum accompanies the wave of phosphatidylcholine synthesis during the G(0) → G(1) transition. *J. Biol. Chem.* **274:** 26240–26248.
28. Lagace, T. A., and N. D. Ridgway. 2005. Induction of apoptosis by

lipophilic activators of CTP:phosphocholine cytidylyltransferase alpha (CCTα). *Biochem. J.* **392:** 449–456.
29. Zacharias, D. A., J. D. Violin, A. C. Newton, and R. Y. Tsien. 2002. Partitioning of lipid-modified monomeric GFPs into membrane microdomains of live cells. *Science.* **296:** 913–916.
30. Esko, J. D., M. M. Wermuth, and C. R. Raetz. 1981. Thermolabile CDP-choline synthetase in an animal cell mutant defective in lecithin formation. *J. Biol. Chem.* **256:** 7388–7393.
31. Cornell, R., and D. E. Vance. 1987. Binding of CTP:phosphocholine cytidylyltransferase to large unilamellar vesicles. *Biochim. Biophys. Acta.* **919:** 37–48.
32. Craig, L., J. E. Johnson, and R. B. Cornell. 1994. Identification of the membrane-binding domain of rat liver CTP:phosphocholine cytidylyltransferase using chymotrypsin proteolysis. *J. Biol. Chem.* **269:** 3311–3317.
33. Johnson, J. E., M. Xie, L. M. Singh, R. Edge, and R. B. Cornell. 2003. Both acidic and basic amino acids in an amphitropic enzyme, CTP: phosphocholine cytidylyltransferase, dictate its selectivity for anionic membranes. *J. Biol. Chem.* **278:** 514–522.
34. Miquel, K., A. Pradines, F. Terce, S. Selmi, and G. Favre. 1998. Competitive inhibition of choline phosphotransferase by geranylgeraniol and farnesol inhibits phosphatidylcholine synthesis and induces apoptosis in human lung adenocarcinoma A549 cells. *J. Biol. Chem.* **273:** 26179–26186.
35. Fornerod, M., M. Ohno, M. Yoshida, and I. W. Mattaj. 1997. CRM1 is an export receptor for leucine-rich nuclear export signals. *Cell.* **90:** 1051–1060.
36. la Cour, T., L. Kiemer, A. Molgaard, R. Gupta, K. Skriver, and S. Brunak. 2004. Analysis and prediction of leucine-rich nuclear export signals. *Protein Eng. Des. Sel.* **17:** 527–536.
37. Cornell, R. B., and I. C. Northwood. 2000. Regulation of CTP:phosphocholine cytidylyltransferase by amphitropism and relocalization. *Trends Biochem. Sci.* **25:** 441–447.
38. Ohba, T., E. C. Schirmer, T. Nishimoto, and L. Gerace. 2004. Energy- and temperature-dependent transport of integral proteins to the inner nuclear membrane via the nuclear pore. *J. Cell Biol.* **167:** 1051–1062.
39. Wu, W., F. Lin, and H. J. Worman. 2002. Intracellular trafficking of MAN1, an integral protein of the nuclear envelope inner membrane. *J. Cell Sci.* **115:** 1361–1371.
40. King, M. C., C. P. Lusk, and G. Blobel. 2006. Karyopherin-mediated import of integral inner nuclear membrane proteins. *Nature.* **442:** 1003–1007.
41. Hinshaw, J. E., B. O. Carragher, and R. A. Milligan. 1992. Architecture and design of the nuclear pore complex. *Cell.* **69:** 1133–1141.
42. Tseu, I., R. Ridsdale, J. Liu, J. Wang, and M. Post. 2002. Cell cycle regulation of pulmonary phosphatidylcholine synthesis. *Am. J. Respir. Cell Mol. Biol.* **26:** 506–515.
43. Wang, Y., and C. Kent. 1995. Identification of an inhibitory domain of CTP:phosphocholine cytidylyltransferase. *J. Biol. Chem.* **270:** 18948–18952.
44. Taneva, S., M. K. Dennis, Z. Ding, J. L. Smith, and R. B. Cornell. 2008. Contribution of each membrane binding domain of the CTP:phosphocholine cytidylyltransferase-α dimer to its activation, membrane binding, and membrane cross-bridging. *J. Biol. Chem.* **283:** 28137–28148.
45. Kitos, T. E., A. Drobnies, M. N. Ng, Y. Wen, and R. B. Cornell. 2006. Contribution of lipid mediators to the regulation of phosphatidylcholine synthesis by angiotensin. *Biochim. Biophys. Acta.* **1761:** 261–271.
46. Peterfy, M., J. Phan, and K. Reue. 2005. Alternatively spliced lipin isoforms exhibit distinct expression pattern, subcellular localization, and role in adipogenesis. *J. Biol. Chem.* **280:** 32883–32889.